The Adriatic Sea General Circulation. Part II: Baroclinic Circulation Structure

A. ARTEGIANI,* D. BREGANT,+ E. PASCHINI,* N. PINARDI,# F. RAICICH,+ AND A. RUSSO*

* *Istituto di Richerche sulla Pesca Marittima, CNR, Ancona, Italy*
+ *Istituto Talassografico di Trieste, CNR, Trieste, Italy*
# *Istituto per lo Studio delle Metodologie Geofisiche Ambientali, CNR, Bologna, Italy*

(Manuscript received 3 March 1995, in final form 5 March 1996)

ABSTRACT

In the second part of the paper dedicated to the Adriatic Sea general circulation, the horizontal structure of the hydrographic parameters and dissolved oxygen fields is described on a seasonal timescale.

Maps of temperature and salinity climatological fields reveal the enhanced seasonal variability of the Adriatic Sea, which at the surface is associated with the major dilution effects of river runoff.

The density and derived dynamic height fields show for the first time the baroclinic geostrophic structure of the general circulation. Winter is dominated by compensation effects between temperature and salinity fronts along the western coastline. The resulting baroclinic circulation is weak and suggests the presence of barotropic current components not accessible by the dataset. Spring and summer seasons have the smallest spatial scales in the temperature and salinity fields and stronger subbasin-scale gyres and current systems, which have been classified in a schematic representation of the circulation. The Adriatic Sea general circulation comprises boundary currents and jets that strengthen and change spatial scales in different seasons. Two separate cyclonic gyres clearly exist in the middle and southern Adriatic except during winter.

The rates of formation of the northern Adriatic deep waters and southern Adriatic deep waters are estimated to be 0.07 and 0.36 Sv (Sv $\equiv 10^6$ m^3 s^{-1}), respectively. Likely driving mechanisms of the circulation are discussed.

1. Introduction

In the first part of this paper (Artegiani et al. 1997, hereafter called Part I) we have presented the air–sea interaction and water mass analysis of the historical hydrological dataset of the Adriatic Sea. The dataset consists of 5543 stations of bottle casts distributed in the periods 1911–14 and 1947–83. The observations comprise temperature, salinity, and dissolved oxygen data. Quality control procedures have been applied to the dataset and are described in section 3 of Part I. Here we consider only stations with casts deeper than 15 m and exclude the eastern basin coastal area stations.

The hydrological variables have been studied on the basis of seasons defined by the annual cycle of heat storage of the basin. In Part I, winter was defined as January–April, spring as May–June, summer as July–October, and autumn as November–December. The annual mean surface heat flux is negative, which must be balanced by an equivalent inflow of heat through the Otranto Channel. The computed climatological freshwater balance indicates that the Adriatic Sea behaves like a dilution basin in all seasons due to river runoff.

We have also defined the climatological water masses and have identified three regions of relatively homogeneous vertical water mass properties: (i) the northern Adriatic Sea, from the 100 m isobath to the northernmost corner of the basin; (ii) the middle Adriatic containing the Pomo Depressions, more than 250 m deep (see Fig. 1 of Part I); and (iii) the southern Adriatic starting approximately from the Pelagosa sill (see Fig. 1 of Part I) to the Otranto Channel. We have analyzed the modified Levantine Intermediate Water (MLIW) of the basin, which appears in the climatological profiles in the middle and southern Adriatic. The deep waters are described as composed principally of northern Adriatic deep water (NAdDW) and southern Adriatic deep water (SAdDW), locally formed in the northern and southern Adriatic, respectively. The deep waters of the middle Adriatic (MAdDW) have also been connected to modified NAdDW.

In this second part, we focus on the climatological baroclinic circulation of the Adriatic Sea, that is, on the dominant horizontal structure of the density-driven circulation as deduced from the seasonal mapping of the hydrological data. The spatial distribution of the hydrological casts used in our analysis is shown in Fig. 1 for each season. The middle and southern Adriatic are

Corresponding author address: Dr. Fabio Raicich, Istituto Sperimentale Talassografico, CNR,Viale Romolo Gessi 2, I-34123 Trieste, Italy.
E-mail: raicich@ts.cnr.it

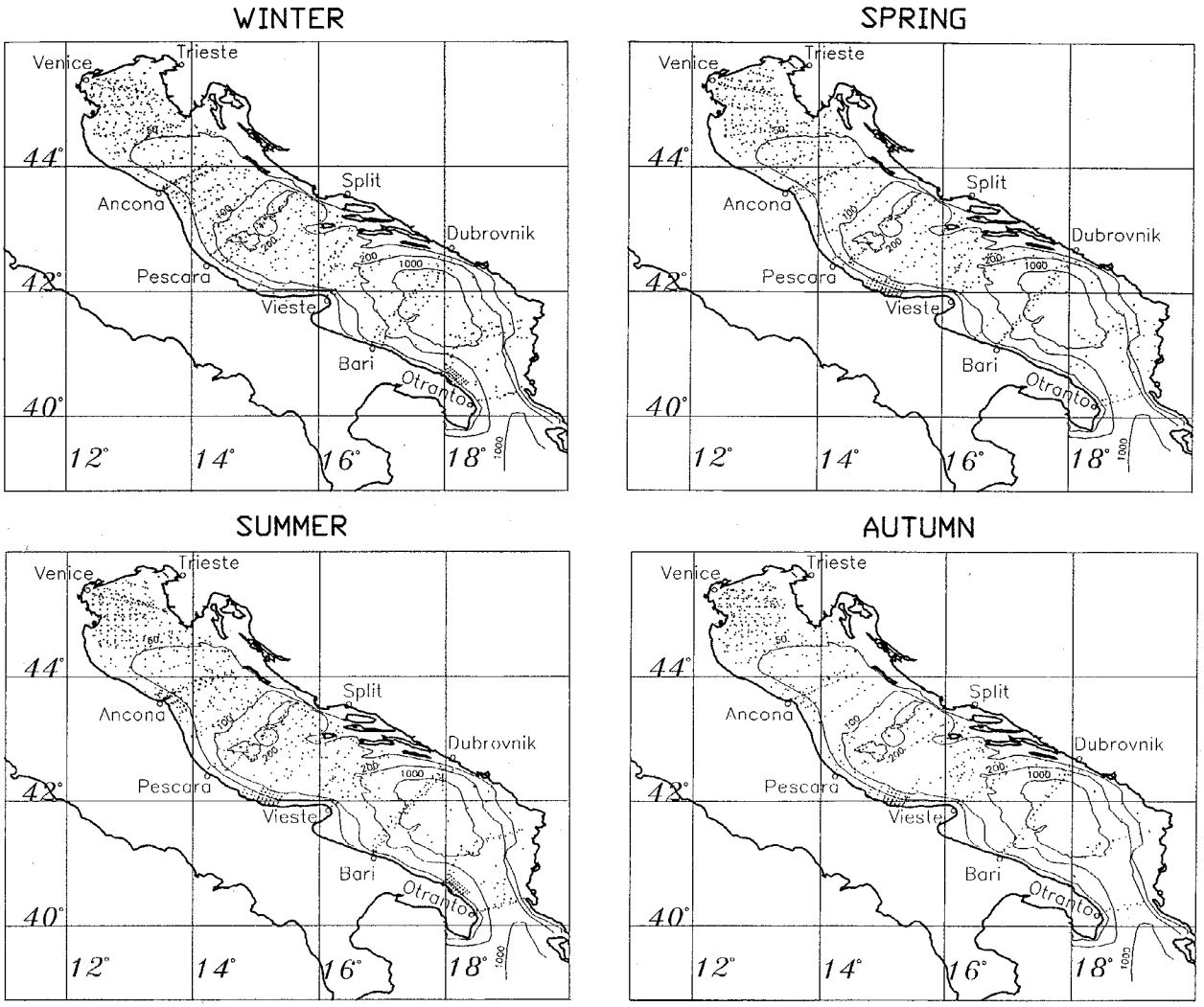

FIG. 1. Seasonal spatial distribution of the casts.

unevenly covered, and during spring and autumn the data are particularly scarce. Although this is the most complete dataset available for the Adriatic Sea, it is insufficient to carry out a monthly analysis of the hydrological parameters. We analyze the horizontal distribution of oxygen saturation percentage, which is used as an indicator of the ''age'' of the deep waters. Oxygen is not a completely passive tracer, but it is the only widely available quantity for the Adriatic at this time.

The Adriatic Sea circulation has been described in the past from the analysis of hydrographic data collected during a limited number of cruises. In the northern Adriatic a cyclonic gyre is reported by Mosetti and Lavenia (1969) in spring and summer 1967, while in spring 1968 it is absent. Small anticyclonic gyres have been found south of the Po River mouth, superimposed on the main flow (Franco 1970), and an anticyclonic circulation is observed by Zore-Armanda and Mladinić (1976) in November 1974. However, these features appear to be rather sporadic in time. The model simulations by Malanotte-Rizzoli and Bergamasco (1983) show the presence of a thermohaline-driven cyclone related to the Po River runoff in summer 1978. A density-driven current is observed along the western coastline in spring. Thus, the northern Adriatic circulation is known to be cyclonic, with intensified jets along the western Adriatic coastlines but seasonally varying in strength. In the middle Adriatic a cyclonic circulation is generally observed in the area of the Pomo Depressions in winter (Zore 1956), spring, and autumn (Zore 1956; Mosetti and Lavenia 1969; Artegiani et al. 1993; Paschini et al. 1993). In summer its position seems to be more variable: between the Pomo Depressions and the western coast (Zore 1956; Mosetti and Lavenia 1969), on the middle axis of the basin (Malanotte-Rizzoli and Bergamasco 1983) and on the eastern Pomo Depression, together with an anticyclone on the western Pomo Depression (Limić and Orlić 1986). Mosetti and Lavenia (1969) observe another cy-

clonic gyre off Ancona in spring and summer 1967. A northern-middle Adriatic western current is reported by Mosetti and Lavenia (1969), Malanotte-Rizzoli and Bergamasco (1983), and Paschini et al. (1993). The connection between the northern and middle Adriatic and the possible interaction between the two cyclonic gyres are unknown. In the southern Adriatic a cyclonic gyre is observed in all seasons (Zore 1956; Limić and Orlić 1986). Zore (1956) reports a relatively strong western coastal current and a weaker eastern current in summer 1911 and 1913, winter 1912, and spring 1913, while in autumn 1913 and winter 1914 the situation appears to be reversed. A well-developed eastern current is reported by Mosetti and Lavenia (1969) in summer 1967 and by Limić and Orlić (1986) in summer 1974. The only information on the baroclinic currents below the sea surface is reported by Paschini et al. (1993), who show the subsurface intensification of the middle Adriatic western current between the Pomo Depressions and the western coastline in autumn 1988.

In this paper we show the observational evidence of the variability of the seasonal general circulation of the overall Adriatic basin. We use the hydrographic dataset studied in Part I and map the water properties at different depths. The dynamic height of the basin is computed separately for the northern region and the remainder of the basin due to the large differences in bottom topography between the different regions.

Much of the scientific attention in the past has concentrated upon the process of deep-water formation occurring in the northern and southern Adriatic. It is well known that dense waters are formed in the Adriatic Sea due to winter heat losses to the atmosphere. Two areas are recognized as places where dense water formation occurs: the northern Adriatic, where a pool of dense water is found, especially in winter and spring (Hendershott and Rizzoli 1976; Malanotte-Rizzoli 1977; Artegiani et al. 1989); and the southern Adriatic (Pollak 1951; Ovchinnikov et al. 1985; Bignami et al. 1990a; Roether and Schlitzer 1991). Some of the dense water found in the middle Adriatic originates from the northern basin (see, for instance, Artegiani and Salusti 1987), but local formation of dense water in the middle Adriatic has been reported by Zore-Armanda (1963). In this paper the dense water distributions in the basin are described, using density and oxygen saturation percentage at the bottom.

In section 2 we describe the horizontal distribution of temperature and salinity properties in the overall basin. In section 3 we describe the bottom density structure of the basin and give estimates of the deep-water formation rates, and in section 4 we show the streamfunction of the geostrophic baroclinic flow field at different depths and present a schematic of the general circulation features. Our results are summarized in section 5.

2. Temperature and salinity fields

In this section, we describe the horizontal structure of the temperature and salinity fields at three different depths, namely, the surface, 100 m, and 200 m, representing the vertical water mass structures of the basin as discussed in Part I. Details on the mapping technique can be found in the appendix.

In Fig. 2a we show the Adriatic Sea surface temperature for the four seasons. Note that seasonal temperature excursions exceed 10°C, clearly due to the heat flux exchanged with the atmosphere. In winter the temperature field exhibits a marked frontal area in the northern region and along the western coast, while it is a rather smooth field in the remaining part of the basin. In summer the surface temperature is rather uniform over the entire Adriatic Sea, but cold and warm centers develop in all the regions. In the transition seasons we clearly recognize smaller spatial structures and enhanced local thermal front areas. We believe that during spring, summer, and autumn the field is actually dominated by mesoscale variability so that our seasonal average is biased by an insufficient amount of data. It is interesting to note that the temperature gradient in the front off the Po River mouth (Fig. 1 of Part I) reaches a maximum in autumn. In this season a large-scale frontal area divides the western and eastern parts of the basin, running along the longitudinal axis of the basin as far south as the Gargano Peninsula (Fig. 1 of Part I). We may speculate that this offshore frontal area retreats toward the western coastlines during winter, forming a well-defined frontal jet along the Italian coast.

Figure 2b illustrates the surface salinity fields. Strong salinity frontal areas can be seen in all the seasons, particularly along the western coast, related to the river runoff. Frontal structures are determined by the strong gradients between the low salinity waters, which are always present along the western side of the Adriatic Sea, and the interior basin salinity field. From spring to summer the relatively fresh waters of the northern Adriatic spread southeastward, intruding into the open sea. Both salinity and temperature fields show large-scale patchiness during the spring–summer seasons, an indication of higher baroclinic eddy activity. The maximum values of salinity are found in winter when the 38.3-psu isohaline includes all the offshore area of the entire basin. Minimum values of salinity occur in summer when the 38.3-psu isohaline encompasses only two small areas in the middle and southern Adriatic. It is interesting to note an area of relatively high salinity (greater than 38.5 psu) in the middle Adriatic, which persists in all seasons. In spring the noticeable influence of the Albanian rivers' runoff is shown by the wide area with salinity less that 38.0 psu in front of the southeastern coastline.

The temperature fields at 100-m depth shown in Fig. 3a are similar to those at the surface only in winter when the water column is homogenized, as shown in Part I. In all the seasons, warmer waters are present on the eastern side of the basin, particularly in autumn, in connection with the development of an eastern current (see section 5). In the middle Adriatic, there is a tem-

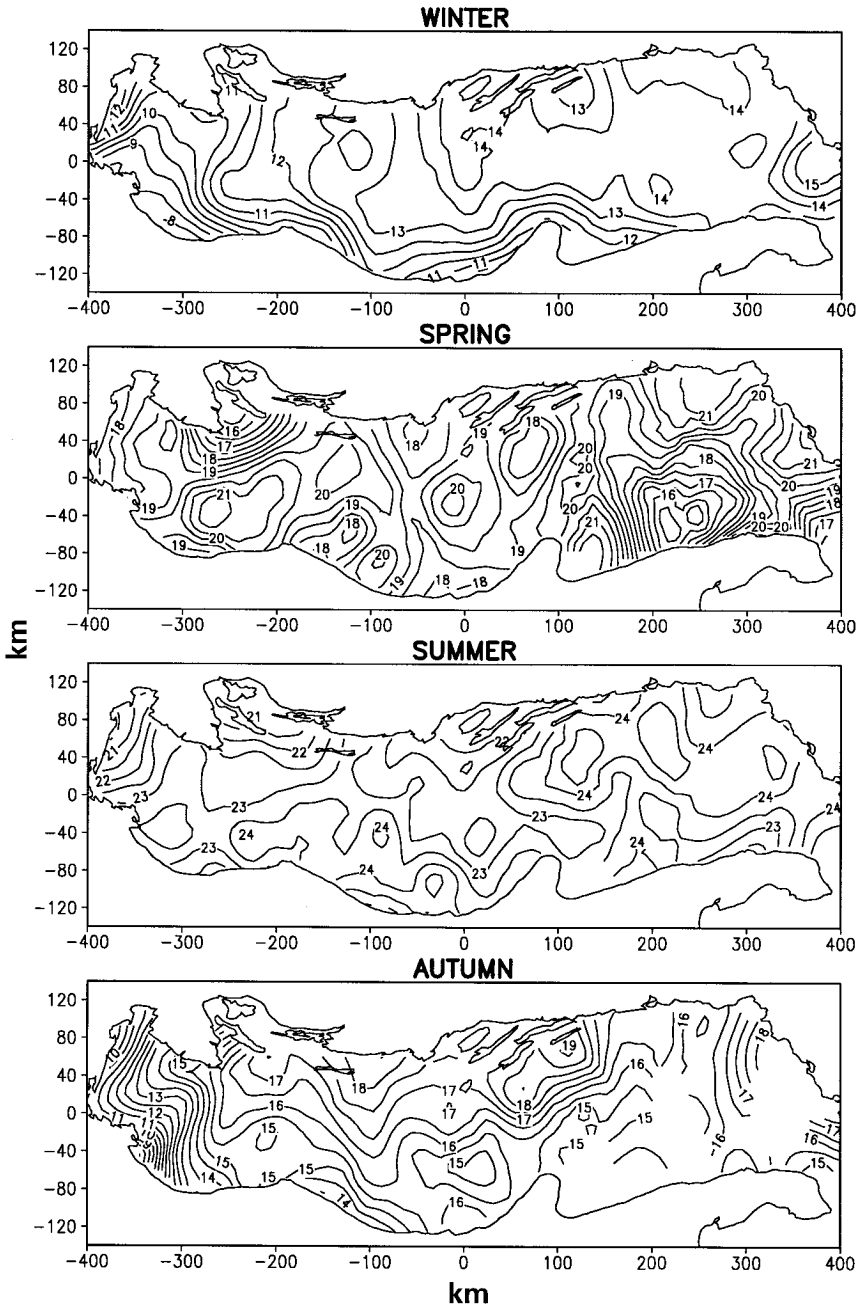

FIG. 2a. Seasonal temperature (°C) maps at the surface. The contour interval is 0.5°C. The field is plotted for expected error less than 30%.

perature minimum in all seasons, with the absolute minimum in winter. If we assume the advective processes to be dominant, the isotherms are shaped as if the NAdDW path into the Pomo Depressions was cyclonic. The salinity fields at 100 m in Fig. 3b do not exhibit any large-scale structure and they are uncorrelated with the surface fields. The ingression of MLIW (see Part I) is evident from spring to autumn, where the 38.6-psu isohaline reaches the middle Adriatic. The analysis of both temperature and salinity fields at 100 m is seriously limited by the incomplete spatial coverage of the southern basin, but it reveals the greater patchiness of the salinity field with respect to temperature.

From Fig. 4a and 4b we can see that at 200-m depth the middle Adriatic depressions are filled with relatively cold ($T < 12$°C in all seasons) waters and that relative minima of temperature and salinity are found in spring and summer in the southern Adriatic. From the salinity distributions we can detect again the ingression of MLIW from Otranto between spring and autumn.

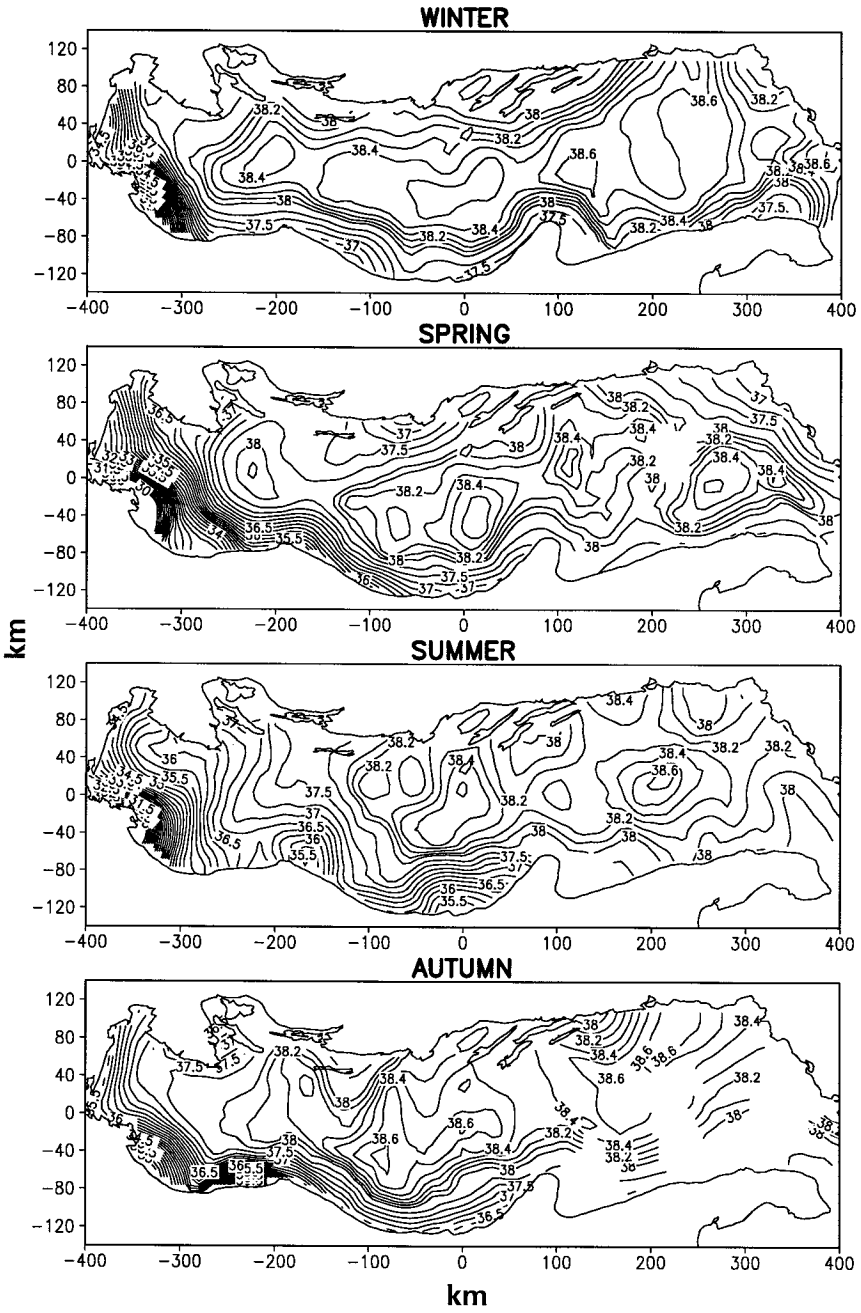

FIG. 2b. Seasonal salinity (psu) maps at the surface. The contour interval is 0.25 psu for $S <$ 38 psu and 0.1 psu for $S >$ 38 psu. Contours for $S <$ 30 psu are not shown. The field is plotted for expected error less than 30%.

3. Bottom waters

The bottom water properties have been deduced from the observations taken in a bottom layer whose thickness is 10% of the water column depth. This choice has been made for the following reasons: (i) the bottom depth has often been measured with unknown but presumably large inaccuracies; (ii) usually, the bottom samples have been taken several meters above the sea floor. Thus, we used the measurements in a bottom layer varying from a few meters to more than 100 m along the variable bottom topography dependant upon total water depth.

Based on the seasonal fields of bottom σ_θ, Fig. 5, relative maxima are present from autumn to spring in the northern Adriatic, with a value greater than 29.4 kg m^{-3} in winter, corresponding to the area of NAdDW formation. Another local maximum is present in the

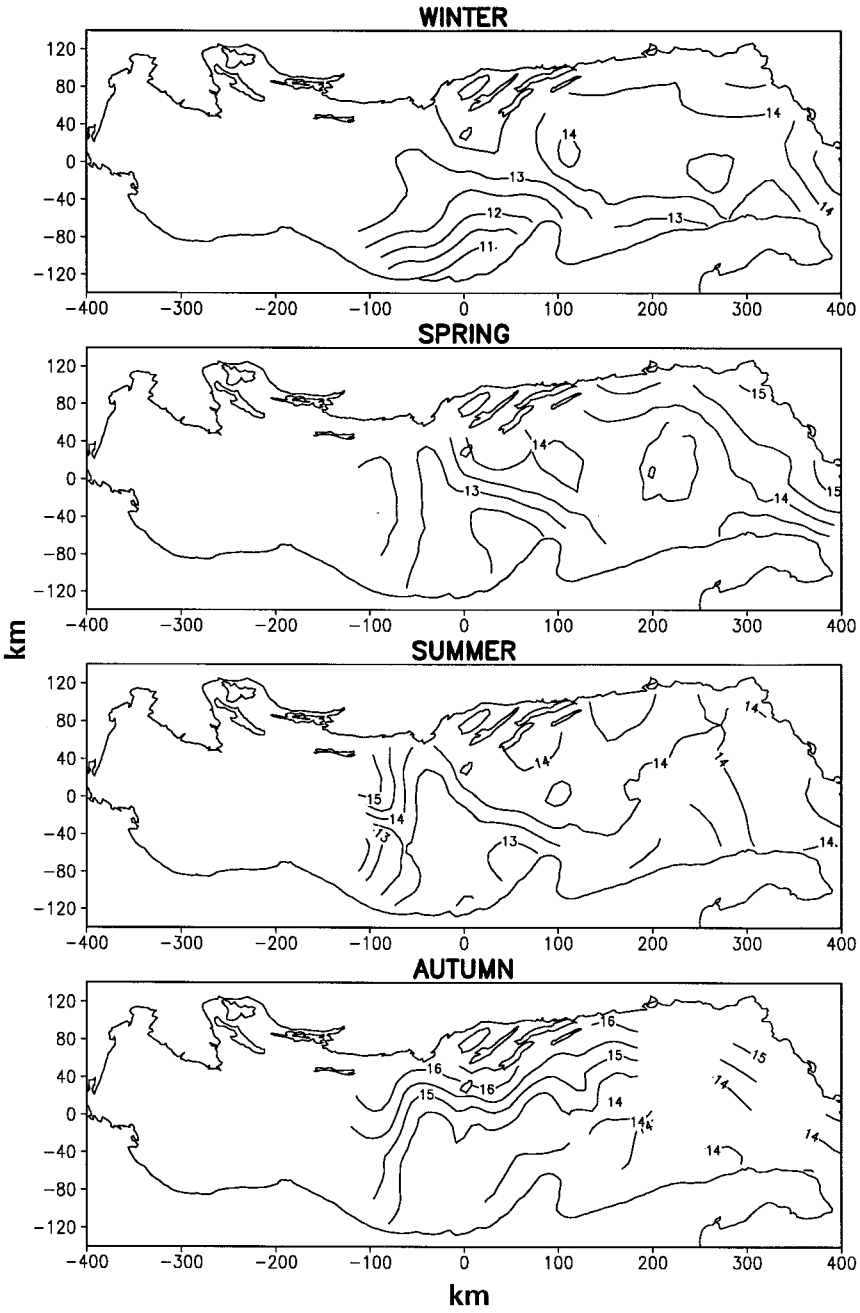

FIG. 3a. Seasonal temperature (°C) maps at 100-m depth. The contour interval is 0.5°C. The field is plotted for expected error less than 30%.

middle Adriatic, at the Pomo Depressions, corresponding to the MAdDW, which is identifiable all year as shown in Part I. In spite of the small amount of data available, there are also indications of a relative maximum in the southern Adriatic. In spring, summer, and autumn, strong gradients occur in the shallow coastal areas, particularly on the western side, mainly related to the fresh waters along the Italian coastline as indicated at the surface in Fig. 2b. It is interesting to note that winter is the only season in which there is no bottom western boundary current in the northern and middle Adriatic. This is an effect of compensation between temperature and salinity that produces no density current on the western boundary of the basin. We can speculate that barotropic motion could be the major component of currents from the surface to the bottom layers during winter.

We estimated the amount of water formed in the Adriatic by two different methods: The first deduces the amount of ''long-living'' deep waters produced each

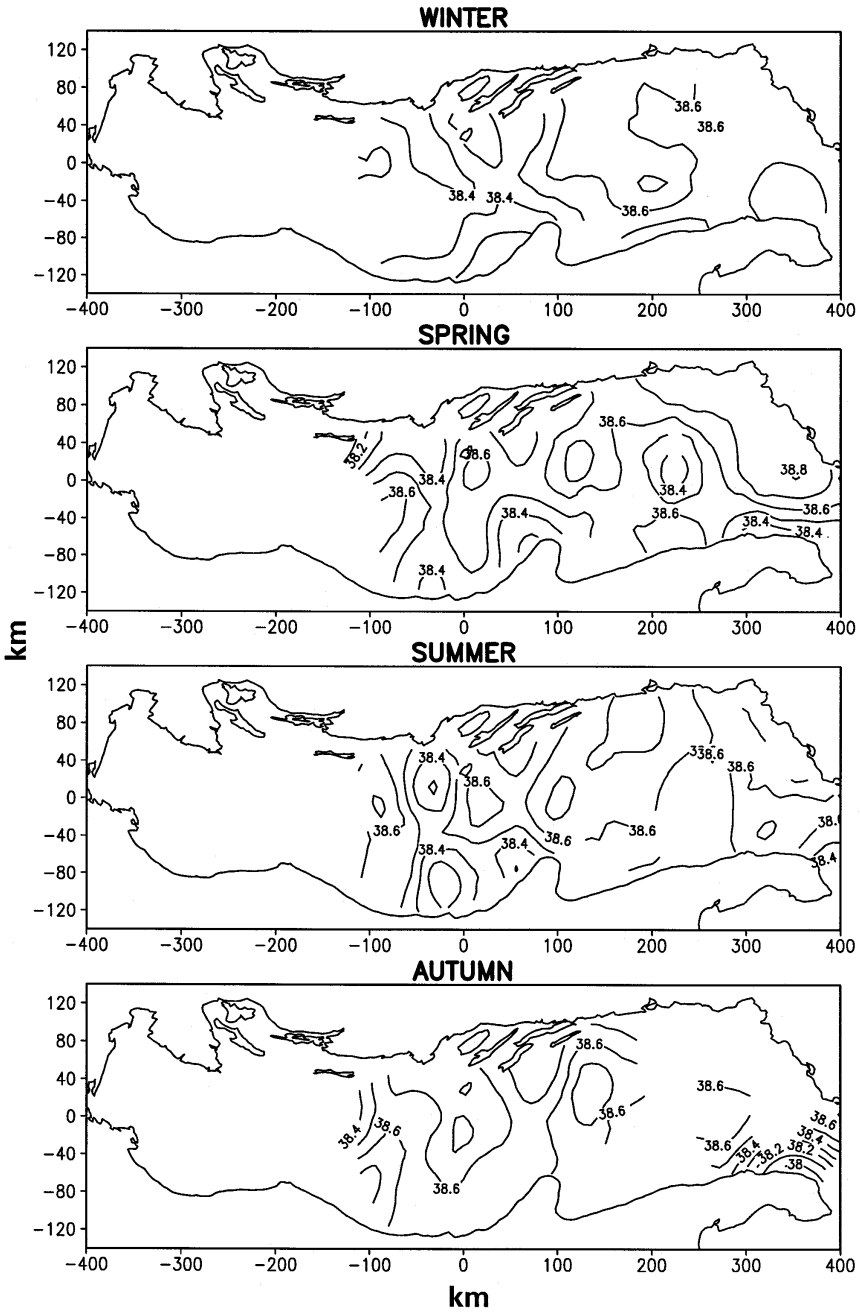

FIG. 3b. Seasonal salinity (psu) maps at 100-m depth. The contour interval is 0.1 psu. The field is plotted for expected error less than 30%.

year from the volume of dense waters found in the deep parts of the basin. These deep waters are ventilated during wintertime and then are left isolated in the deep (or arrive in the region by advection/diffusion) and do not come into contact with the atmosphere anymore. Using this method, the pool of MAdDW ($\sigma_t > 29.2$ kg m^{-3}) covers an area of approximately 9900 km^2 at the end of summer and extends from the bottom up to about 150-m depth, as seen from Fig. 12 of Part I. If we assume that this water is totally renewed every year, we compute that 0.007 Sv of waters are formed or advected to the middle Adriatic bottom areas. An analogous computation for the southern Adriatic indicates that the SAdDW ($\sigma_t > 29.1$ kg m^{-3}) covers an area of about 18 500 km^2 and extends vertically from the bottom to a depth of about 400 m, corresponding to an annual production rate of 0.3 Sv (Sv $\equiv 10^6$ m^3 s^{-1}).

The second method uses heat and water fluxes to compute the buoyancy flux and the associated cross-isopycnal flux, defined in terms of Sverdrups (Speer and

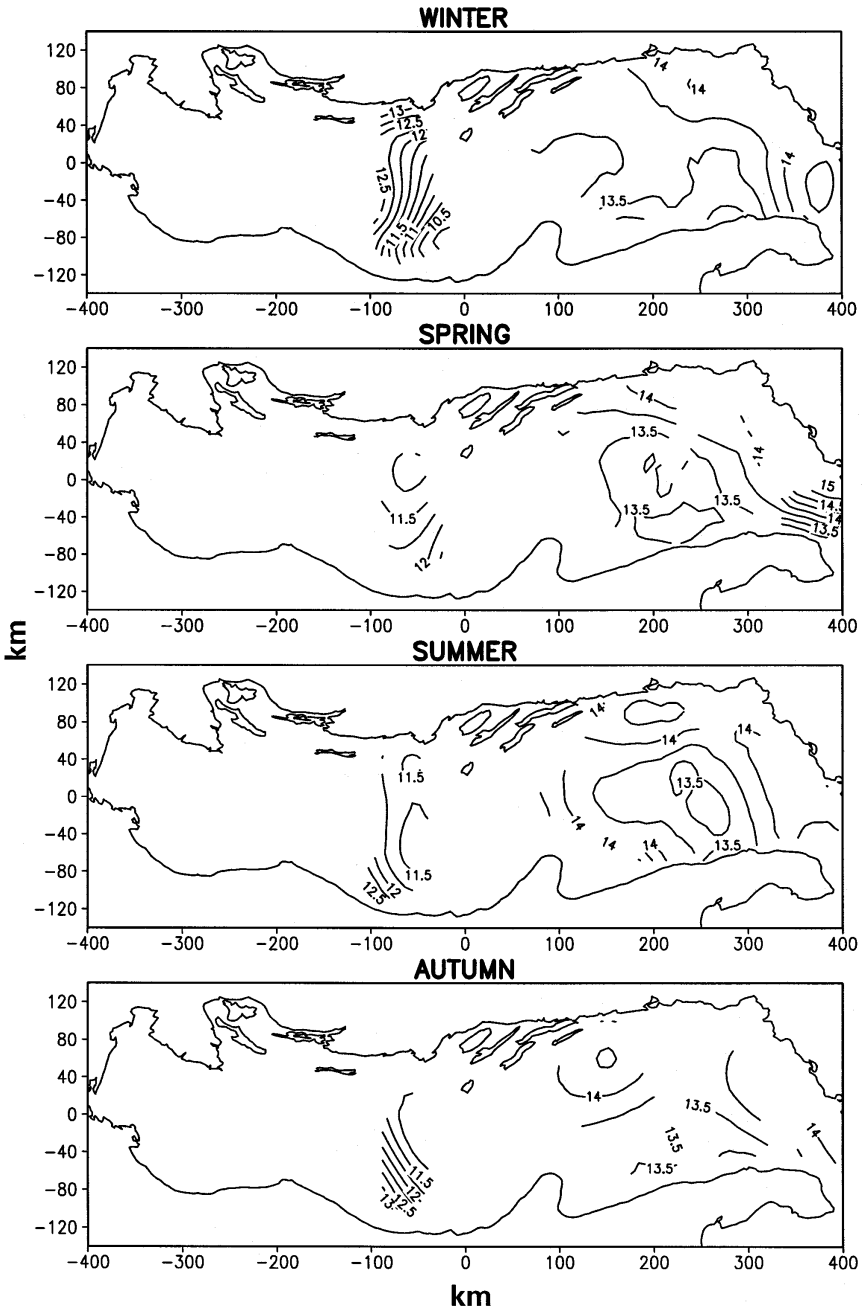

FIG. 4a. Seasonal temperature (°C) maps at 200-m depth. The contour interval is 0.25°C. The field is plotted for expected error less than 30%.

Tziperman 1992; Lascaratos 1993). This method gives an estimate of the newly formed water each year by the climatological surface forcing. On the basis of these estimates we calculated the following:

1) In the northern Adriatic 0.07 Sv of dense waters are formed with $\sigma_t > 29.2$ kg m^{-3}.
2) In the middle Adriatic 0.002 Sv of dense waters are formed with $\sigma_t > 29.2$ kg m^{-3}.
3) In the southern Adriatic we estimate 0.36 Sv of dense waters are formed with $\sigma_t > 29.0$ kg m^{-3}.

We have computed the production rates by means of different heat and water flux datasets, namely, those described in section 2 of Part I. The quantitative results given above represent the maximum estimated rate and have been obtained using the heat fluxes derived from the NMC meteorological data.

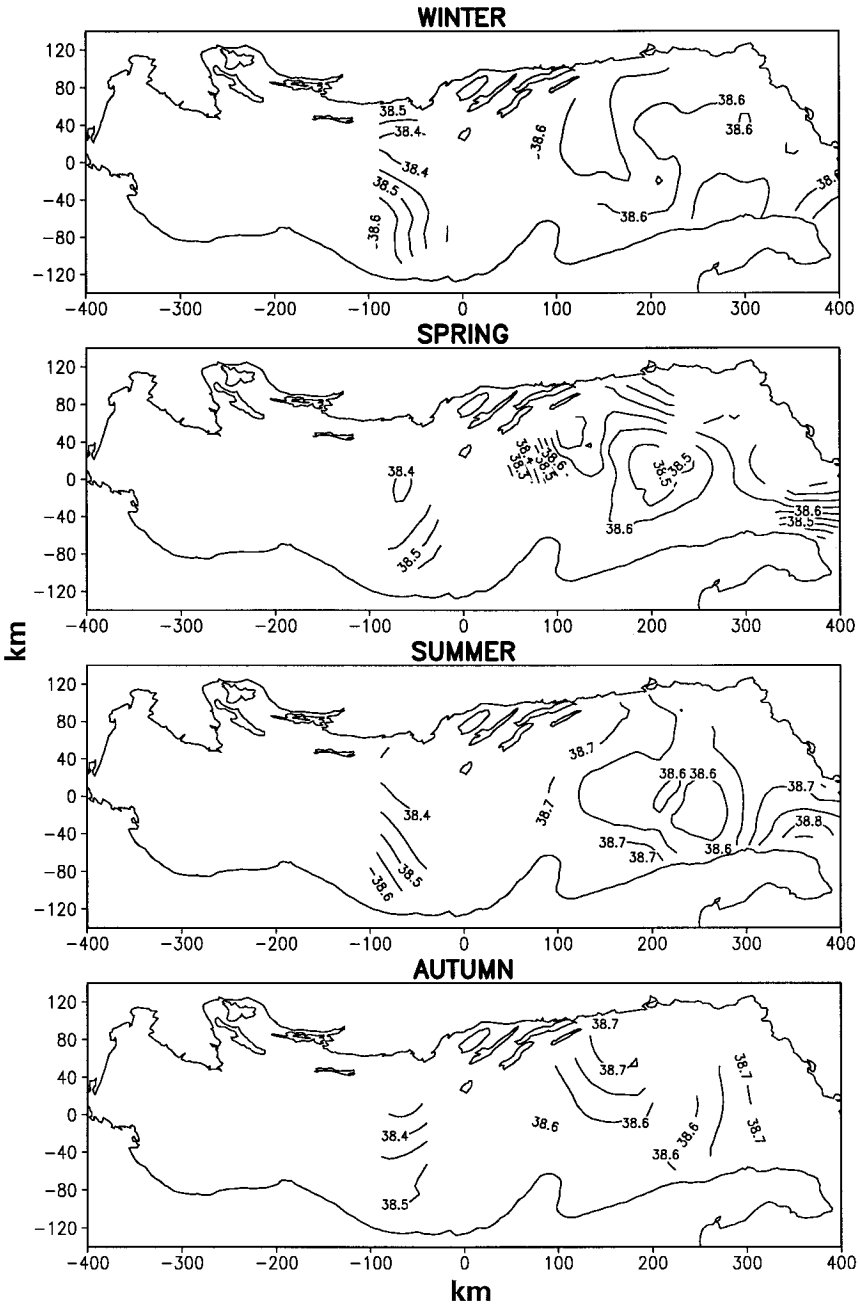

FIG. 4b. Seasonal salinity (psu) maps at 200-m depth. The contour interval is 0.05 psu. The field is plotted for expected error less than 30%.

We must observe that the amount of MAdDW formed from the surface flux computations is lower than the corresponding volume of waters found in the depressions. Thus, we conclude that approximately two-thirds of MAdDW are advected from the northern regions, as qualitatively discussed in Part I. The calculations of the formation rate of NAdDW indicate that less than 10% of the volume of deep waters formed is stored in the middle Adriatic depressions and the rest is either retransformed locally or exported throughout the remaining part of the basin.

Furthermore, we note that our estimate of SAdDW formation rates from surface fluxes is in agreement with the long-lived deep water budget only if the density threshold is 29.0 kg m^{-3}. If we take the ventilated isopycnal to be 29.1 kg m^{-3}, then only 0.04 Sv are formed. Thus, we speculate that a contribution to the deep water pool of the southern Adriatic could come from the mid-

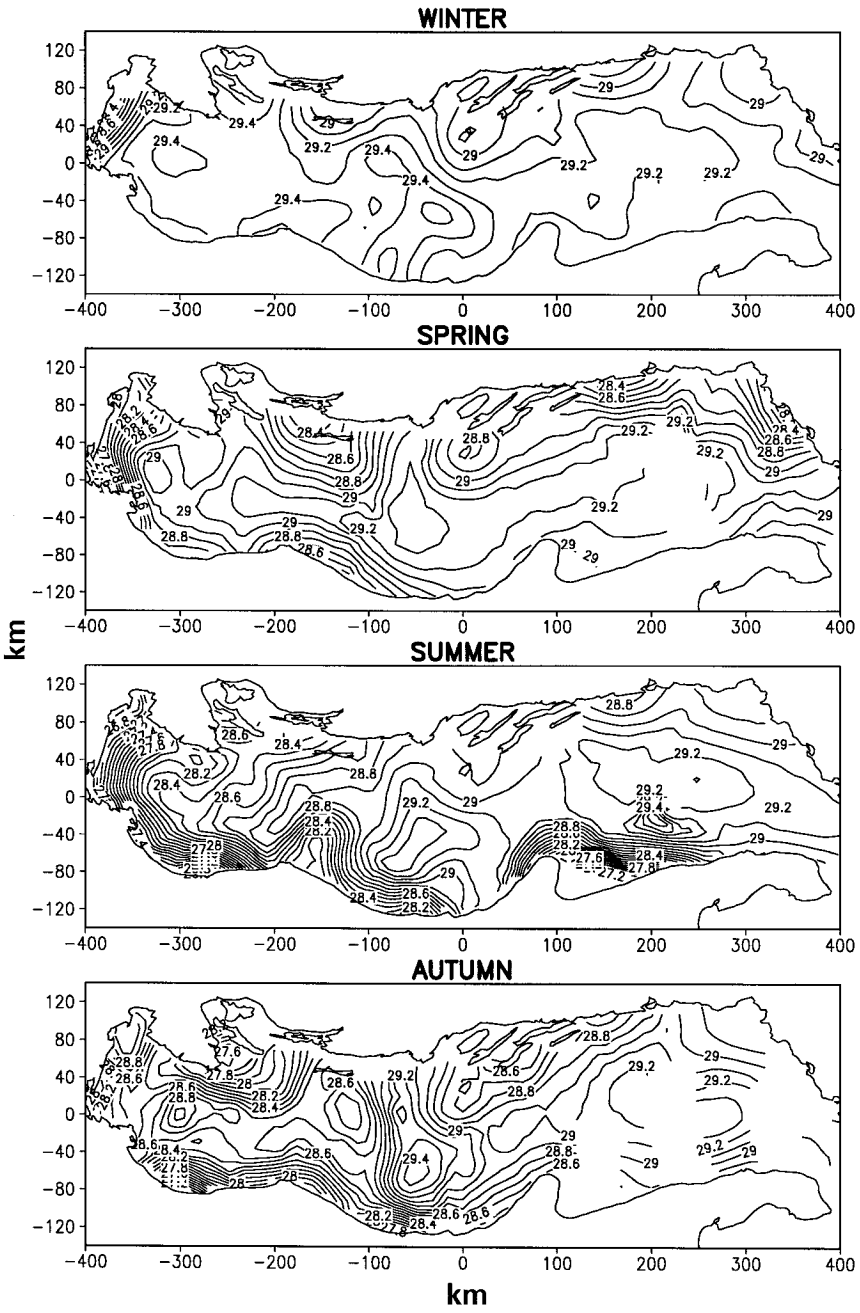

FIG. 5. Seasonal maps of bottom σ_θ (kg m^{-3}). The contour interval is 0.1 kg m^{-3}. The field is plotted for expected error less than 30%.

dle and northern Adriatic deep waters (Bignami et al. 1990b) or from nonclimatological forcing factors affecting the rates of formation. The estimated SAdDW formation rate is consistent with that of 0.29 ± 0.09 Sv of deep waters exiting the Otranto Channel made by Roether and Schlitzer (1991) but smaller than that evaluated by Ovchinnikov et al. (1985), who reported 0.75 Sv.

The maps of Fig. 6 show a minimum of bottom oxygen saturation percentage near the Po River mouth in spring and summer. Oxygen is, in fact, consumed by the oxidation of organic matter but is not supplied at the same rate because the water column stratification severely limits ventilation of the bottom layer. The high oxygen saturation percentage during winter in the northern Adriatic is another indication of the deep-water formation processes occurring there. From winter to spring the oxygen saturation percentage increases slightly, probably due to warming of the lower layers of the water column. In fact, given a constant dissolved oxygen con-

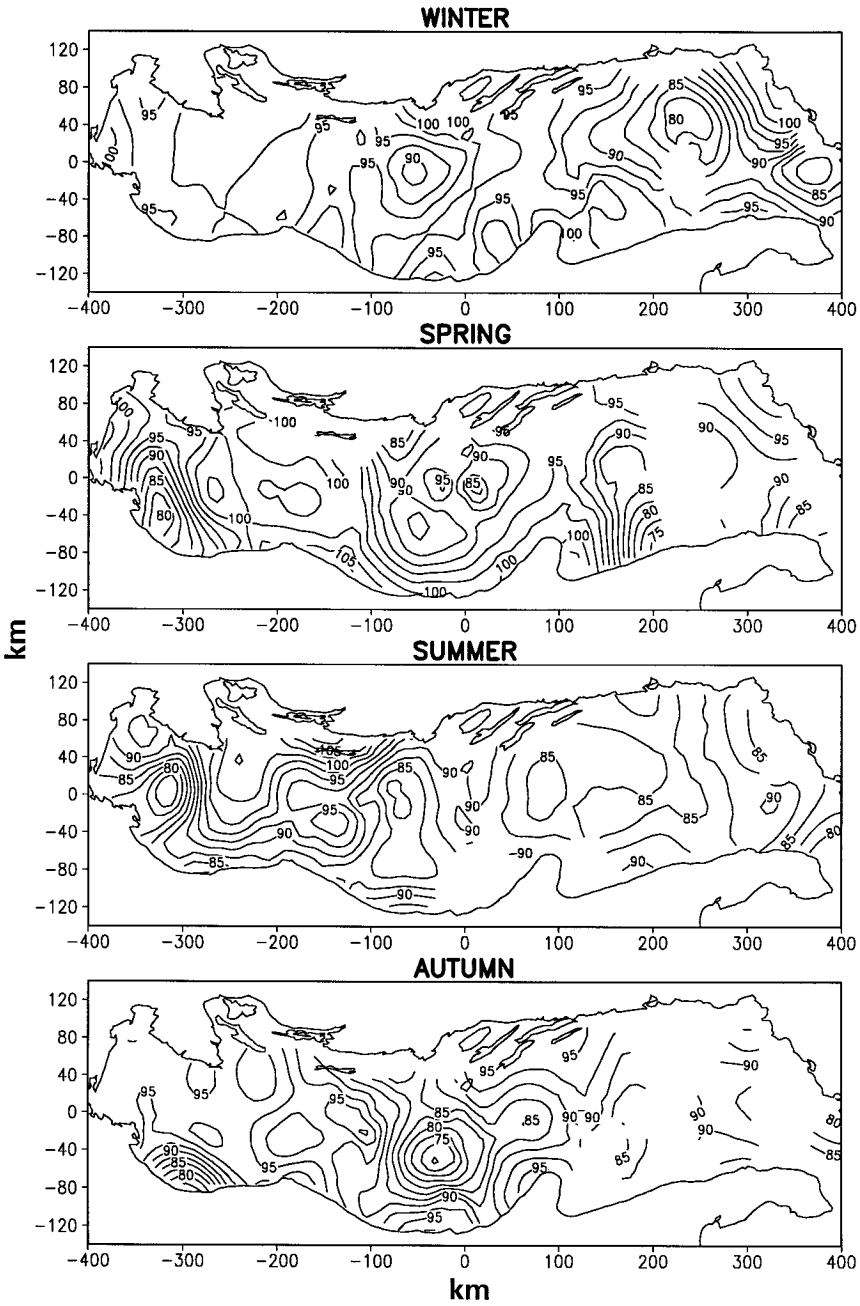

FIG. 6. Seasonal maps of bottom oxygen saturation percentage. The contour interval is 5%. The field is plotted for expected error less than 30%.

centration when temperature increases, the oxygen saturation percentage increases too; as we know from Part I, in spring there is a 1°–2°C increase of the bottom temperature in the northern Adriatic. The relatively low saturation percentage found in the middle Adriatic depressions can be mainly explained by the presence of MAdDW, which is probably mostly modified NAdDW. The slow oxygen depletion in the middle Adriatic can be interpreted as aging of the waters, being determined by oxygen consumption due to biogeochemical processes in the absence of an oxygenated water source.

4. Dynamic height fields

In this section we present a description of the baroclinic general circulation structure for the entire basin. Dynamic height anomalies have been calculated relative to the annual-mean dynamic height for each season.

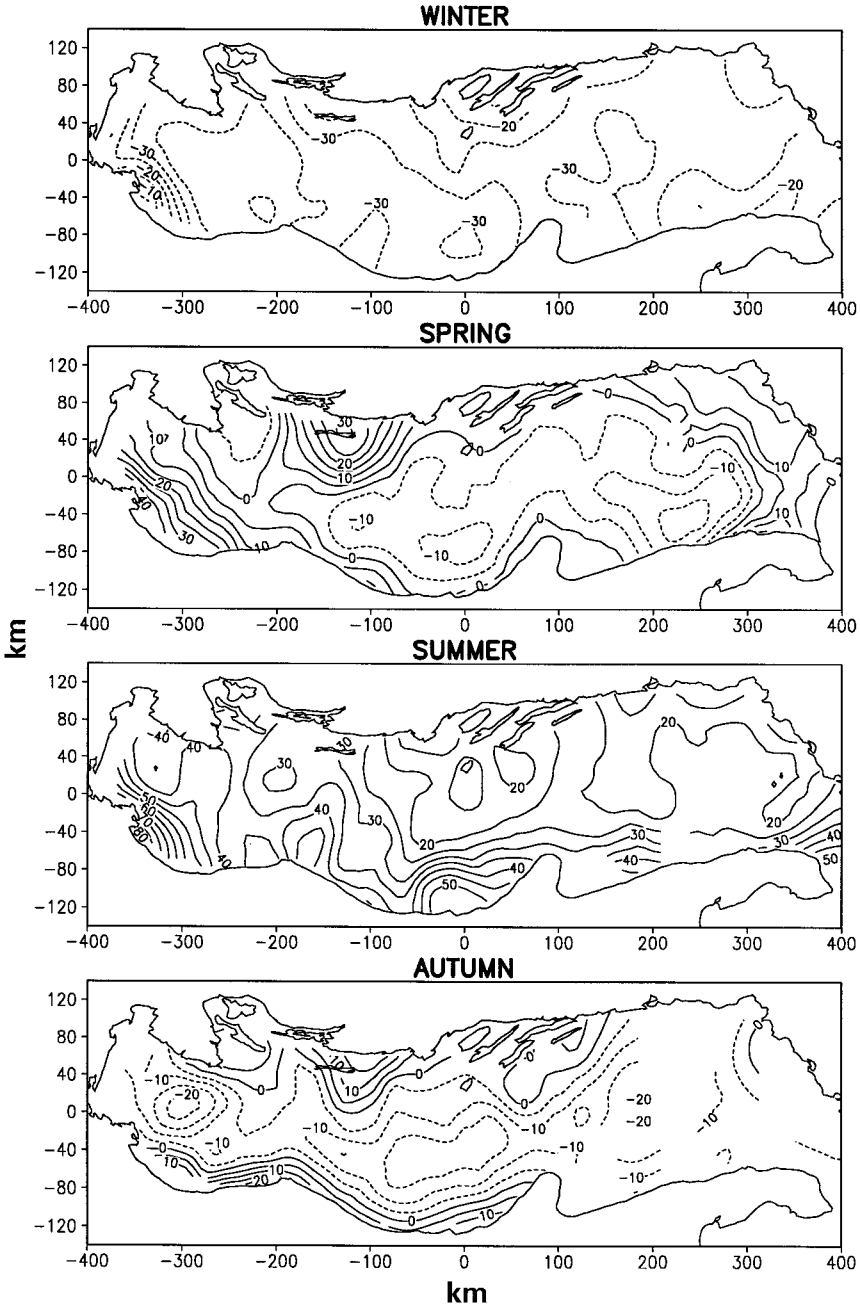

FIG. 7a. Seasonal maps of dynamic height anomalies (dyn mm) at 0 m relative to 30 m. The contour interval is 5 dyn mm and the dotted lines indicate negative values. The field is plotted for expected error less than 30%.

Due to the shallowness of the northern and middle Adriatic we had to use two different reference levels. The first is located at 30 m, approximately the average bottom depth of the northern Adriatic, and the second is at 140 m, near the bottom depth of the shallower part of the middle Adriatic.

First, the surface northern Adriatic circulation is described as shown in Fig. 7a. A prominent structure of the circulation is given by a northern Adriatic current (NAd current), which is observed in front of the Po River mouth. During winter the NAd current is a segment off the Po River mouth extending only 100 km downstream. During spring the current broadens in the northern part and extends farther south. In this season it flows along the Italian coastline up to the middle of the southern Adriatic with local intensification. The segment of this current in the middle Adriatic is called the western-middle Adriatic current (W-MAd current) since

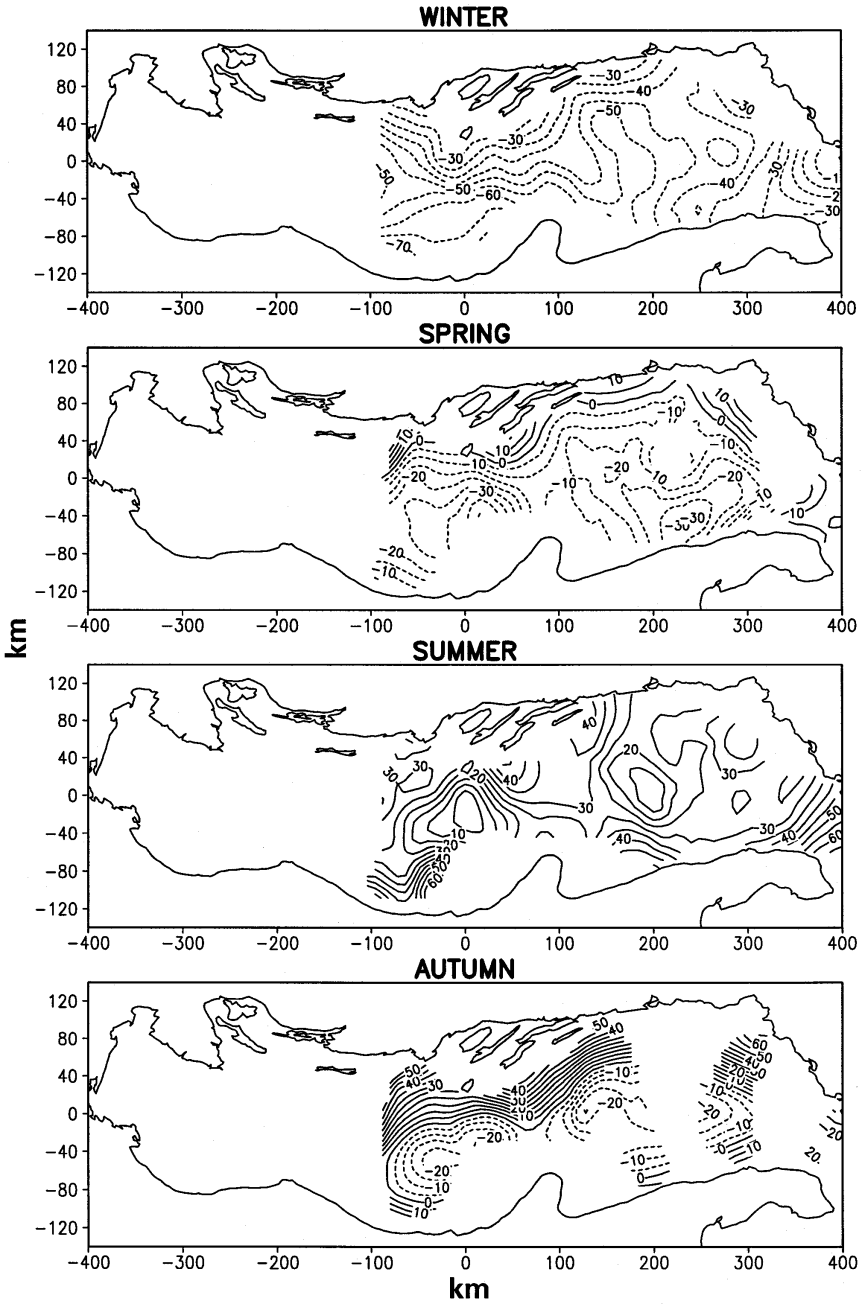

FIG. 7b. Seasonal maps of dynamic height anomalies (dyn mm) at 0 m relative to 140 m. The contour interval is 5 dyn mm and the dotted lines indicate negative values. The field is plotted for expected error less than 30%.

in summer it appears separated from the NAd current. Between spring and summer the NAd and W-MAd currents broaden and meander offshore, intruding almost to the midlongitudinal axis of the basin. In autumn the NAd and W-MAd currents rejoin to form an extended boundary current along the Italian coastline. The density-driven circulation in the northern and middle Adriatic is then weak during winter, and we expect barotropic or vertically homogeneous motion to prevail. Another prominent feature of the circulation is the northern Adriatic cyclonic gyre (NAd gyre), becoming evident in summer and autumn at the surface. From our analysis, it is clear that the baroclinic structure of this gyre is purely seasonal.

In conclusion, the northern Adriatic surface circulation is dominated by the NAd current, which exhibits a significant seasonal variability, and the NAd gyre, defined mainly in autumn. Due to the shallowness of

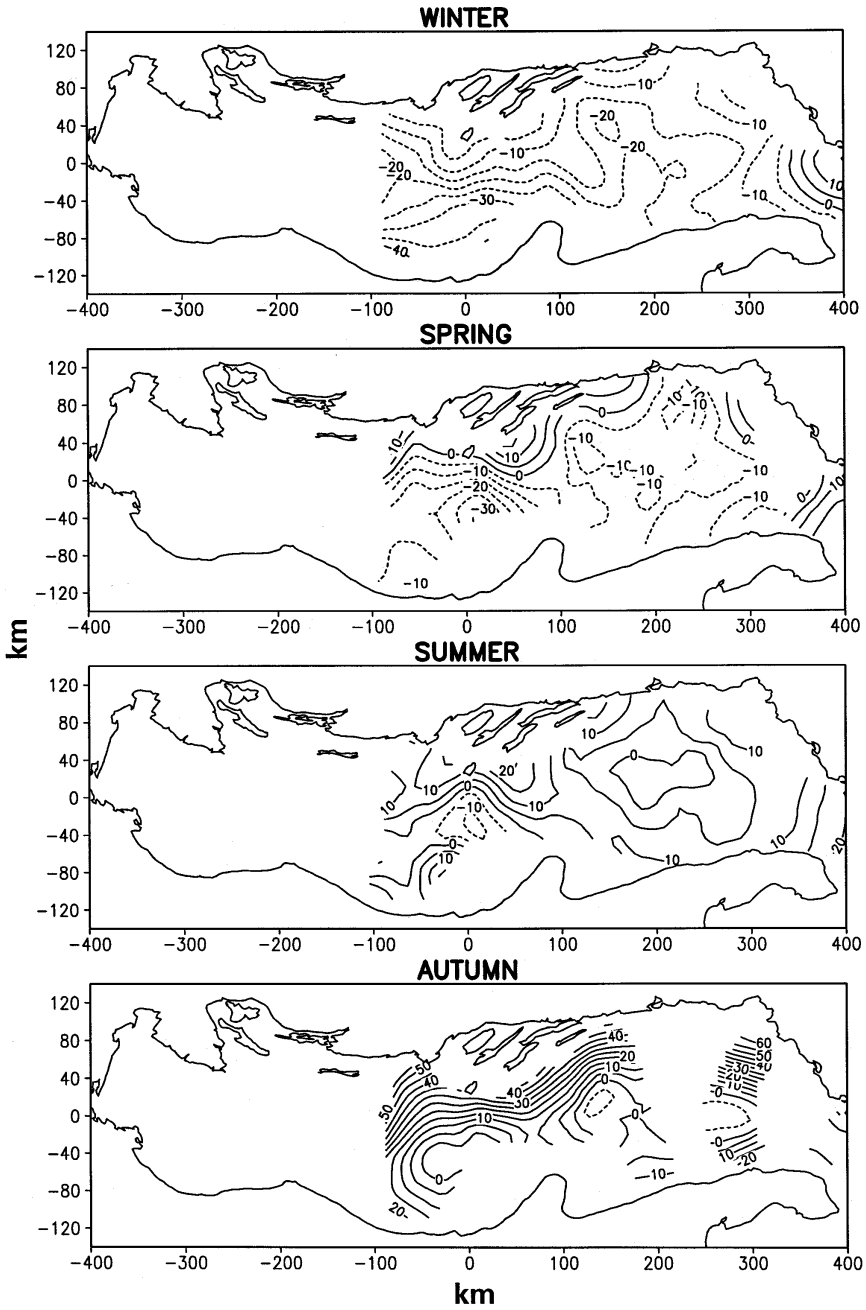

FIG. 7c. Seasonal maps of dynamic height anomalies (dyn mm) at 30 m relative to 140 m. The contour interval is 5 dyn mm and the dotted lines indicate negative values. The field is plotted for expected error less than 30%.

the reference level chosen we cannot draw, from Fig. 7a, any definitive conclusion about the middle and southern Adriatic circulation. However, there is evidence that a unique western boundary intensified current is present only in autumn along the Italian coastline. We also found that the baroclinic component of the general circulation is weak in the winter season, as expected, due to the uniformity of the vertical profiles and it strengthens considerably during the remaining seasons due to restratification of the water column.

We describe now the surface circulation for the middle and southern Adriatic by showing in Figs. 7b and 7c the dynamic height referenced to the 140-m depth. The dynamic height at 0 and 30 m are very similar and they will be discussed together hereafter. The seasonal character is a very prominent feature of the circulation, which is composed of the middle Adriatic and south

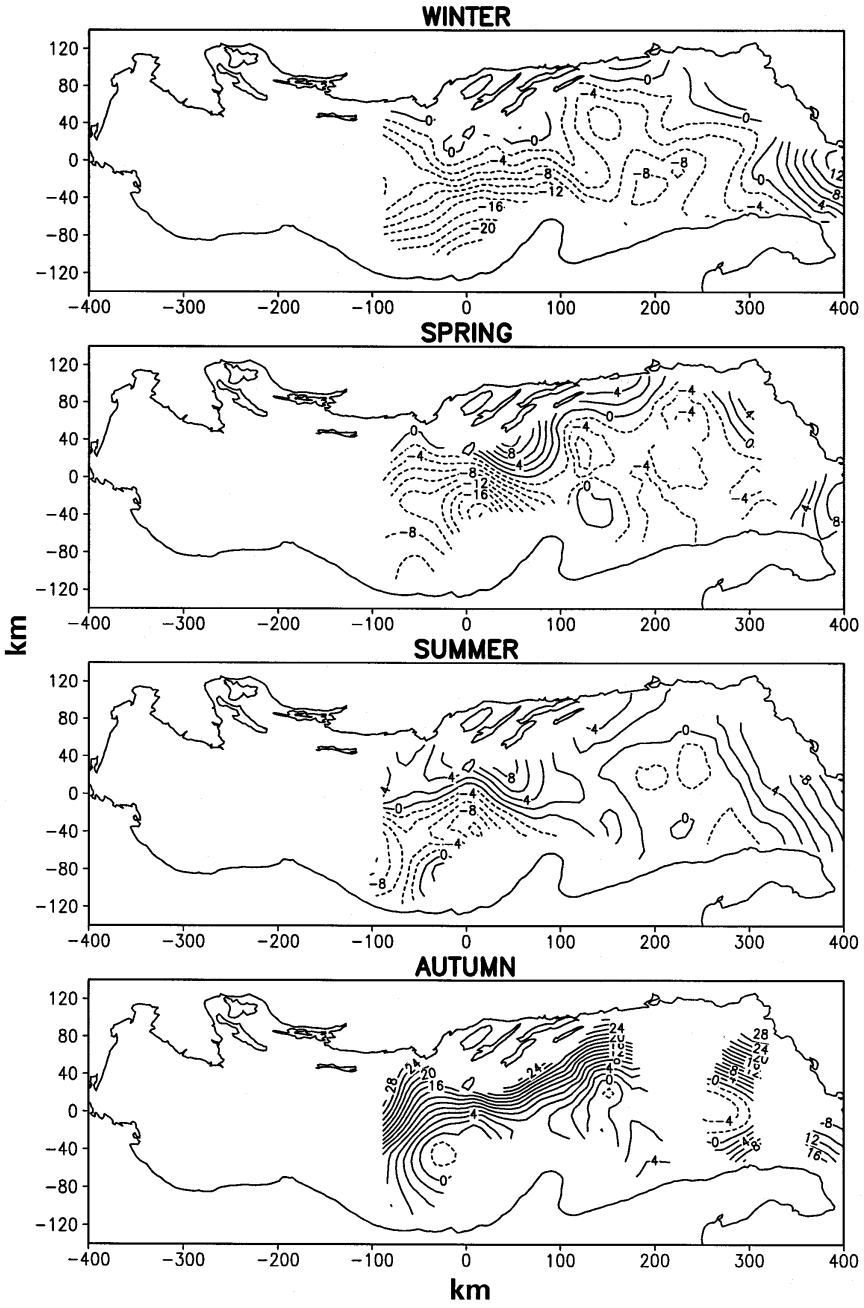

FIG. 7d. Seasonal maps of dynamic height anomalies (dyn mm) at 75 m relative to 140 m. The contour interval is 2 dyn mm and the dotted lines indicate negative values. The field is plotted for expected error less than 30%.

Adriatic gyres (MAd and SAd gyres), an eastern south Adriatic current (E-SAd current), and a western south Adriatic current (W-SAd current). These four features of the circulation strengthen during summer, while they are weaker in spring and almost absent in winter. During winter, in fact, the field is less energetic and dominated by a smooth flow from south to north along the longitudinal center of the basin. We may speculate that the return flow is confined in a very narrow region along the Italian coastline, which we do not capture because of the deep reference level. In summary, the surface baroclinic circulation apparently requires an alongshore shelf flow to close the circulation cyclonically during winter.

Summer and autumn show evidence of the intensification of both the surface MAd and SAd gyres. During summer we see segments of W-MAd and W-SAd currents extending as far as Otranto. The W-MAd current

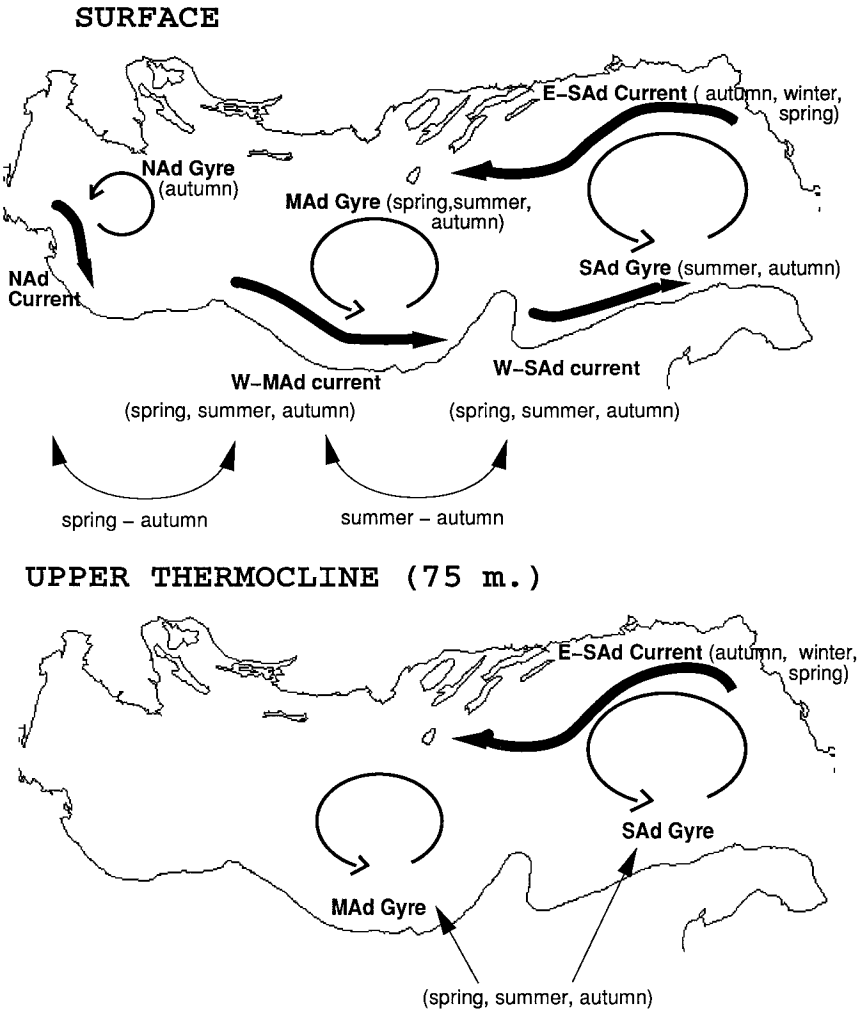

FIG. 8. Schematics of the Adriatic Sea baroclinic circulation.

persists throughout the autumn when the MAd and SAd gyres reach maximum amplitude and definition. At that time the E-SAd current is also well defined, occupying a large portion of the eastern regions of the basin.

In Fig. 7d we show the upper thermocline structure of the general circulation for the middle and southern Adriatic represented by the dynamic height at 75-m depth referred to 140 m. As for the surface, the MAd and SAd gyres are defined from spring to autumn together with the E-SAd current, which is also related to the maximum advection of MLIW in the basin (see Part I). The winter flow field is weaker, generally cyclonic in the south. In this season again the thermocline flow field seems to be dominated by a broad northward current along the longitudinal center of the basin, with a possible return flow along the shelf areas of the basin.

We have synthesized the structure and seasonal variability of the Adriatic general circulation in Fig. 8. At the surface the winter general circulation is composed only of NAd and SAd current segments and the flow field is very different from all other seasons. The general circulation is dominated by temperature and salinity compensation effects, which give no resulting density signal. We may speculate that the barotropic, wind-induced transport and circulation is probably a major component of the general circulation during winter. This also could have been estimated by looking at the seasonal water mass properties of Part I, where during winter and throughout the basin the vertical temperature and salinity profiles become practically uniform with depth (small or zero baroclinic Rossby radius of deformation).

The spring–summer surface flow field is characterized by the appearance of western current segments (W-MAd, W-SAd currents) and the two major cyclonic gyres of the Adriatic circulation. We argue that the seasonal vertical stratification in the basin triggers the appearance at the surface of gyres and boundary intensifications, more generally of eddies and jets, probably a result of baroclinic/barotropic nonlinear instabilities in the basin. During summer the smallest spatial scales

occur and the E-SAd current weakens. The autumn conditions are characterized by maximum spatial coherence in the general circulation structure. In fact, there are three cyclonic gyres, a continuous western Adriatic boundary current, connected between the three subbasins, and an intense SAd current. As known from Part I, this season has maximum MLIW entrance and spreading from Otranto, a well-defined surface mixed layer, and maximum warming of the subsurface layers of the northern Adriatic. The aggregation of the general circulation into large-scale structures could be due both to the stabilization of the water column and to the structure of the external forcing of the circulation. We believe that the Otranto inflow of MLIW could be a substantial part of that external forcing. The wind driving during autumn also consists of a southeasterly wind, called ''scirocco,'' which in turn could reinforce the inflow of water at Otranto.

At the depth of the seasonal thermocline (75 m) we can define the presence in certain seasons of the E-SAd current and the SAd gyre. The MAd gyre is not evident at this depth during winter as is the case for the surface flow field. The spring–summer flow field is again characterized by smaller spatial scales than in the other two seasons. It is interesting to note that a weak anticyclonic circulation area is present during spring–summer south of the Vieste section (see Part I).

5. Conclusions

This second part of the paper has shown the observational evidence for the space–time scales of the Adriatic Sea general circulation. The large-scale temperature and salinity distributions have been mapped by means of traditional objective analysis. The largest-scale temperature frontal area is along the western coastline during winter and along the longitudinal axis of the basin during autumn. The low salinity frontal area due to river runoff is concentrated along the western basin shelf–slope area and is present in all seasons. Spring and summer seasons show small spatial scales both for temperature and salinity, an indication of enhanced baroclinic dynamics in the basin.

The deep water oxygen distribution has been shown to clearly mark the NAdDW and MAdDW located in the northern Adriatic and in the Pomo Depressions, respectively. The northern Adriatic shows the largest rate of oxygen consumption in the basin due to biochemical processes, with an absolute maximum of such activity off the Po River delta.

Deep water formation rates have been estimated by means of surface heat and water fluxes and compared with the water volumes occupying the deep parts of the basin, enabling us to argue that the NAdDW is not only advected into the middle Adriatic depressions, but may also contribute to the SAdDW pool.

The baroclinic general circulation has been classified into currents and gyres. The strength and occurrence of these structures is seasonal, especially in the northern and middle Adriatic Sea. The wintertime conditions are characterized in the first 100 m of depth by a wide northward flow field, probably associated with intense but shallow return jets along the western coastline, while in the other seasons coastal currents develop, particularly in autumn along the eastern coast.

The spring–summer and autumn conditions show elements of well-known circulation patterns in the basin. Here we have identified for the first time their occurrence and their changes in a seasonal progression. The western side of the Adriatic basin is a site of intense current segments, which are disconnected in the three subbasins (northern, middle, and southern) in spring and summer. The autumn conditions show an overall cyclonic circulation with the intensification of three cyclonic gyres in the subbasins.

From this description we can clearly depict that the forcing of the general circulation has three major components, perhaps equally important for the overall Adriatic dynamical engine. The first component is river runoff, characterized by the low salinity waters derived mainly from the Po and Albanian Rivers. The Po forcing produces compensation of temperature and salinity gradients horizontally and is an important component of the buoyancy budget in the overall basin. In fact, we have an overall heat loss together with a water gain, in contrast to the overall Mediterranean, which exhibits a water loss. The second component is the wind and heat forcing at the surface, which produce deep-water masses in the northern and southern Adriatic and forces the circulation to be seasonal. The third component is the Otranto Channel forcing, which inputs heat and salt in the circulation as a restoring mechanism for the northern heat losses and water gains.

Modeling studies should now be able to elucidate the relative importance of these three forcings on the general circulation. Further observational studies need to resolve the mesoscale variability of the basin, probably more intense during spring–summer, and the relative energy content of the barotropic components of the general circulation.

Acknowledgments. This research has been undertaken in the framework of the Mediterranean Targeted Project (MTP)—MERMAIDS II Project, and finished during the Mediterranean Targeted Project phase II—MATER. We acknowledge the support of the European Commission's Marine Science and Technology Programme (MAST II and III), Contracts MAS2-CT93-0055 and MAS3-CT96-0051. We thank Prof. A. Lascaratos for interesting comments on the deep-water production rates. We thank also Dr. J. Baretta, Dr. P. Radford, Dr. M. Zavatarelli, and Prof. G. Mellor for helpful comments on the manuscript. Thanks are also due to Mr. P. Carini for his assistance in figure drawing.

APPENDIX

The climatological maps shown in Figs. 2, 3, 4, 5, 6, and 7 have been produced by means of an objective analysis technique developed after the works by Gandin (1965), Bretherton et al. (1976), and Carter and Robinson (1987). The interpolation has been made according to the optimal linear estimation theory, based on the Gauss–Markov theorem. The β-plane approximation has been made so that the origin of the coordinate system is located at 42.87°N, 15.87°E and the coordinates (x, y) are measured in kilometers. The mapping domain is tilted by 43.5° counterclockwise with respect to the south–north direction.

The adopted correlation function is isotropic and has the following expression:

$$C(r) = (1 - r^2/a^2)\exp(-r^2/2b^2),\ r^2 = x^2 + y^2,$$

where a is the zero-crossing distance and b the spatial decay scale. These parameters should meet the condition $a > 2^{1/2}b$ to generate a positive-definite correlation matrix. Since we are interested in the analysis of climatological fields, we have chosen $a = 100$ km, approximately half the transverse size of the basin, and $b = 60$ km, based upon Robinson et al. (1991).

The observational noise is approximated by an error variance of 10%. The map has been blanked where the expected error variance exceeds 30%, indicating that we are not confident enough with the interpolated results. All the observations closer to each other less than 12 km have been preliminarily averaged in order to avoid very high correlations. The number of influential points is chosen to be 10 and the mapping resolution is 8 km in both coordinates. The total domain consists of 800 $\times$ 280 km^2 and 101 $\times$ 36 points, 1972 of which are points located in the Adriatic Sea.

REFERENCES

Artegiani, A., and E. Salusti, 1987: Field observation of the flow of dense water on the bottom of the Adriatic Sea during the winter of 1981. *Oceanol. Acta,* **10,** 387–392.

——, R. Azzolini, and E. Salusti, 1989: On the dense water in the Adriatic Sea. *Oceanol. Acta,* **12,** 151–160.

——, M. Gačić, A. Michelato, V. Kovačević, A. Russo, E. Paschini, P. Scarazzato, and A. Smirčić, 1993: The Adriatic Sea hydrography and circulation in Spring and Autumn (1985–1987). *Deep-Sea Res. II,* **40,** 1143–1180.

——, D. Bregant, E. Paschini, N. Pinardi, F. Raicich, and A. Russo, 1997: The Adriatic Sea general circulation. Part I: Air–sea interactions and water mass structure. *J. Phys. Oceanogr.,* **27,** 1492–1514.

Bignami, F., E. Salusti, and S. Schiarini, 1990a: Observations on a bottom vein of dense water in the southern Adriatic and Ionian Seas. *J. Geophys. Res.,* **95,** 7249–7259.

——, G. Mattietti, A. Rotundi, and E. Salusti, 1990b: On a Sugimoto–Whitehead effect in the Mediterranean Sea: Sinking and mixing of a bottom current in the Bari Canyon, southern Adriatic Sea. *Deep-Sea Res.,* **37,** 657–665.

Bretherton, F. P., R. E. Davis, and C. B. Fandry, 1976: A technique for objective analysis and design of oceanographic experiments applied to MODE-73. *Deep-Sea Res.,* **23,** 559–582.

Carter, E. F., and A. R. Robinson, 1987: Analysis models for the estimation of oceanic fields. *J. Atmos. Oceanic Technol.,* **4,** 49–74.

Franco, P., 1970: Oceanography of northern Adriatic Sea. 1 Hydrologic features: Cruises July–August and October–November 1965. *Archo Oceanol. Limnol.,* **XVI** (Suppl. 1), 1–93.

Gandin, L. S., 1965: *Objective Analysis of Meteorological Fields.* Israel Program for Scientific Translations, 242 pp.

Hendershott, M. C., and P. Rizzoli, 1976: The winter circulation in the Adriatic Sea. *Deep-Sea Res.,* **23,** 353–373.

Lascaratos, A., 1993: Estimation of deep and intermediate water mass formation rates in the Mediterranean Sea. *Deep-Sea Res. II,* **40,** 1327–1332.

Limić, N., and M. Orlić, 1986: Objective analysis of geostrophic currents in the Adriatic Sea. *Geofizika,* **3,** 75–84.

Malanotte-Rizzoli, P., 1977: Winter oceanographic properties of Northern Adriatic Sea. Cruise January–February 1972. *Arch. Oceanogr. Limnol.,* **19,** 1–45.

——, and A. Bergamasco, 1983: The dynamics of the coastal region of the northern Adriatic Sea. *J. Phys. Oceanogr.,* **13,** 1105–1130.

Mosetti, F., and A. Lavenia, 1969: Ricerche Oceanografiche in Adriatico nel periodo 1966–1968. *Boll. Geofis. Teor. Appl.,* **11,** 191–218.

Ovchinnikov, I. M., V. I. Zats, V. G. Krivosheia, and A. I. Udodov, 1985: Formation of deep Eastern Mediterranean waters in the Adriatic Sea. *Oceanology,* **25,** 704–707.

Paschini, E., A. Artegiani, and N. Pinardi, 1993: The mesoscale eddy field of the middle Adriatic during fall 1988. *Deep-Sea Res. I,* **40,** 1365–1377.

Pollak, M. J., 1951: The sources of deep water of the Eastern Mediterranean Sea. *J. Mar. Res.,* **10,** 128–152.

Robinson, A. R., M. Golnaraghi, W. G. Leslie, A. Artegiani, A. Hecht, E. Lazzoni, A. Michelato, E. Sansone, A. Theocharis, and Ü. Ünlüata, 1991: The Eastern Mediterranean general circulation: Features, structure and variability. *Dyn. Atmos. Oceans,* **15,** 215–240.

Roether, W., and R. Schlitzer, 1991: Eastern Mediterranean deep water renewal on the basis of cholorofluoromethane and tritium data. *Dyn. Atmos. Oceans,* **15,** 333–354.

Speer, K., and E. Tziperman, 1992: Rates of water mass formation in the North Atlantic Ocean. *J. Phys. Oceanogr.,* **22,** 93–104.

Zore, M., 1956: On gradient currents in the Adriatic Sea. *Acta Adriat.,* **8,** 1–38.

Zore-Armanda, M., 1963: Les masses d'eau de la mer Adriatique. *Acta Adriat.,* **10,** 1–94.

——, and G. Mladinić, 1976: Some results of direct current measurements in the north-west part of the Adriatic Sea (in Croatian, with abstract in English). *Hidrografski Godišnjak 1974,* 61–67.